A Simplified Meshless Method for Dynamic Crack Growth

Y.Y Zhang and L. Chen

Abstract: A simplified meshless method for dynamic crack growth is presented. The method uses an extrinsic enrichment based on a local partition of unity concept. The crack is represented by a set of crack segments. The crack segments are required to pass through the entire domain of influence of node. They are introduced when the maximum principal stress exceeds the uniaxial tensile strength. The crack segments are allowed to rotate in order to avoid too stiff system responses. The major advantage of our method is that it does not require algorithms to track the crack path.

Keyword: meshless, crack, enrichment, fracture

1 Introduction

Dynamic fracture is of interest in many industrial applications, e.g. Earthquake Engineering, design of armor, break of glass (windows), to name a few. Numerical simulation of dynamic fracture still remains a challenge. Particular difficulties occur due to the huge amount of cracking under dynamic loading. If dynamic fracture is to be modelled realistically, it is essential to model the initiation, propagation and coalescence of cracks. Finite element methods are not well suited for this task since cracks can only occur along element interfaces. This requires computational expensive remeshing algorithms and is only feasible for few cracks. Recent developments of finite element methods allow arbitrary crack growth. However, due to the complexity of the crack representation, these methods are only suitable for a few number of cracks. Smeared crack models Zimmermann (1986); Bazant and Oh (1983); Jirasek and Zimmermann (1998); Malvar and Fourney (1990) are principally able to deal with large amount of

cracks. However, as the name might indicate, they cannot describe the crack properly. Therefore, they are not well suited for dynamic fracture modelling.

Meshless methods have proven to be a powerful alternative to finite element methods Sladek, V. Sladek, and Zhang (2007); Wu and Tao (2007); Han and Atluri (2004); Rabczuk and Eibl (2003); Han, Liu, Rajendran, and Atluri (2007); Wen and Hon (2007); Shen and Atluri (2005); Idelsohn, Onate, and Pin (2004); Rabczuk, Belytschko, and Xiao (2004); Hao and Liu (2006). They were pioneered by Atluri and Zhu (1998, 2000); Atluri and Shen (2002), Belytschko, Lu, and Gu (1994); Belytschko and Tabbara (1996); Belytschko, Krongauz, Organ, Fleming, and Krysl (1996), Liu, Jun, and Zhang (1995) and other, see e.g. Duarte and Oden (1996); Melenk and Babuska (1996). They were applied to various problems involving non-linear material Nishioka, Kobayashi, and Fujimoto (2007); Rabczuk and Belytschko (2005), thermo-mechanical Chen, Gan, and Chen (2008) and piezo-electrical analysis Nguyen-Van, N, and Tran-Cong (2008); Wu and Liu (2007), contact Guz, Menshykov, and Zozulya (2007), beams Andreaus, Batra, and Porfiri (2005), plates Mai-Duy, Khennane, and Tran-Cong (2007) and shells Rabczuk and Areias (2006); Rabczuk, Areias, and Belytschko (2007a); Wu and Liu (2007) as well as fracture Sladek, Sladek, and Zhang (2007); Hagihara, Tsunori, and Ikeda (2007); Guo and Nairn (2006); Hao, Liu, and Chang (2000); Rabczuk and Belytschko (2006); Fujimoto and Nishioka (2006); Gao, Liu, and Liu (2006); Rabczuk and Zi (2007); Zi, Rabczuk, and Wall (2007); Sladek, Sladek, and Krivacek (2005); Nishioka, Tchouikov, and Fujimoto (2006); Le, Mai-Duy, and Tran-Cong (2008); Liu, Long, and Li (2008), shear bands Rabczuk, Areias, and Belytschko (2007b); Hao,

Liu, and Qian (2000) and multiscale analysis Ma, Lu, and Wang (2006); Liu, Hao, and Belytschko (1999); Haasemann, Kastner, and Ulbricht (2006). An excellent state-of-the-art textbook about meshless methods, their applications and abilities is given in Atluri (2002). Cracks can be easily incorporated in meshless methods due to the absence of a mesh Belytschko and Lu (1995); Belytschko, Lu, and Gu (1995); Hao, Liu, Klein, and Rosakis (2004); Li and Simonson (2003); Han and Atluri (2003); Tang, Shen, and Atluri (2003); Liu, Han, Rajendran, and Atluri (2006). Typical methods in order to obtain a discontinuous displacement field across the crack surface are the visibility method Belytschko, Lu, and Gu (1995), the diffraction method and the transparency method Organ, Fleming, Terry, and Belytschko (1996). However, these methods are also suitable for small number of cracks.

All these methods require a representation of the crack surface. That makes these methods difficult to implement with increasing numbers of cracks. Therefore, we propose a meshless method that does not need crack representation but that simultaneously is capable of capturing the discontinuous displacement field. This is accomplished by representing the crack as a set of crack segments. These crack segments pass through the entire domain of influence of the nodes. The discontinuous displacement field is obtained by an extrinsic enrichment based on a local partition of unity concept.

In linear elastic fracture mechanics, the singularity dominates the stress field around the crack tip. Stress intensity factors or the energy release rate is used as failure criterion. However, linear elastic fracture mechanics is only applicable to very brittle materials. If nonlinear material behavior is to be modeled, different approaches have to be used. Cohesive zone models Barenblatt (1962); Hillerborg, Modeer, and Peterson (1976) are commonly used to describe the post-localization behavior. This is necessary for materials with strain softening since the use of pure continuum models lead to mesh dependent results Bazant and Belytschko (1985). We will use cohesive zone models in our meshless crack segment method.

2 Meshless Method

Meshless methods are based only on nodal approximations. We use the element-free Galerkin (EFG) method. The shape functions are obtained by Moving Least Square (MLS) approximation. The EFG approximation is written in terms of a polynomial basis $\mathbf{p}(\mathbf{X})$ and unknown coefficients $\mathbf{a}(\mathbf{x})$:

$$\mathbf{u}^{con}(\mathbf{X},t) = \sum_i p_i(\mathbf{X})\, a_i(\mathbf{X}) = \mathbf{P}^T(\mathbf{X})\, \mathbf{a}(\mathbf{X}) \qquad (1)$$

where $\mathbf{p}$ is a polynomial basis; here chosen to be linear $\mathbf{p}^T(\mathbf{X}) = (1, X, Y)$ since the linear basis guarantees conservation of linear momentum and angular momentum. Minimization of a discrete weighted $\mathscr{L}_2$ error norm J with respect to the unknown coefficients $\mathbf{a}$

$$J = \sum_I \left(\mathbf{P}^T(\mathbf{X}_I)\, \mathbf{a}(\mathbf{X}_I) - \mathbf{u}_I\right)^2 w(\mathbf{X} - \mathbf{X}_I, h) \qquad (2)$$

leads to the final EFG approximation

$$\mathbf{u}^{con}(\mathbf{X},t) = \sum_{I \in \mathscr{W}} N_I(\mathbf{X})\mathbf{u}_I(t) \qquad (3)$$

with the EFG shape functions

$$N_I(\mathbf{X}) = \mathbf{p}^T(\mathbf{X})\, A^{-1}(\mathbf{X})\, \mathbf{D}_I(\mathbf{X}) \qquad (4)$$

and

$$\begin{aligned} \mathbf{D}_I(\mathbf{X}) &= w(\mathbf{X} - \mathbf{X}_I, h)\mathbf{p}^T(\mathbf{X}_I) \\ \mathbf{A}_I(\mathbf{X}) &= \sum_I w(\mathbf{X} - \mathbf{X}_I, h)\, \mathbf{p}(\mathbf{X}_I)\, \mathbf{p}^T(\mathbf{X}_I) \end{aligned} \qquad (5)$$

The superscript *con* in eq. (3) denotes the continuous displacement field; $w(\mathbf{X} - \mathbf{X}_I, h)$ is the so-called Lagrangian weighting function and h is the interpolation radius of this weighting function. For dynamic fracture, it is important to express all quantities in material coordinates $\mathbf{X}$ instead of spatial coordinates $\mathbf{x}$ as commonly done in SPH-methods Randles and Libersky (1997); Rabczuk and Eibl (2003). Belytschko, Guo, Liu, and Xiao (2000) have shown that the use of Eulerian weighting functions can lead to artificial fracture.

3 Displacement Field

Crack is a strong discontinuity in the displacement field. It is captured by decomposing the displacement field into a continuous and discontinuous part:

$$\mathbf{u}(\mathbf{X}) = \underbrace{\mathbf{u}^{con}(\mathbf{X})}_{\text{continuous}} + \underbrace{\mathbf{u}^{dis}(\mathbf{X})}_{\text{discontinuous}} \tag{6}$$

The continuous approximation was given in the previous chapter. The discontinuous approximation will be explained subsequently.

The displacement approximation is based on a local partition of unity method. Additional degrees of freedoms used to describe the crack kinematics are added only around the crack. This minimizes computational cost. Instead of describing the crack as continuous line, we propose to model the discrete crack by cohesive crack segments that pass through the domain of influence of node, figure 1. This avoids the need of tracking the crack path. Complicated phenomena such as branching cracks can be treated with ease and good accuracy. The discontinuous displacement approximation that is active only for nodes that contain the cohesive crack segments is given by:

$$\mathbf{u}^{dis}(\mathbf{X}) = \sum_{I \in \mathscr{W}_c} N_I(\mathbf{X}) \, \Psi(\mathbf{X}) \, \mathbf{q}_I \tag{7}$$

where $\mathscr{W}_c$ are the nodes where the cohesive crack segments pass through, $\mathbf{q}_I$ are additional unknowns and $\Psi(\mathbf{X})$ is the enrichment function describing the crack kinematics. It is required that the crack segments pass through the node but with adaptive methods, crack segments can be introduced anywhere in the solid. To capture the correct crack kinematics, Ψ is the step function

$$\Psi(\mathbf{X}) = \begin{cases} 1 & \text{if } \mathbf{n} \cdot (\mathbf{X} - \mathbf{X}_I) > 0 \\ -1 & \text{if } \mathbf{n} \cdot (\mathbf{X} - \mathbf{X}_I) < 0 \end{cases} \tag{8}$$

Note that only cracked nodes are enriched. The length of the cohesive segment is equal to the size of the domain of influence of the associated cracked node. The jump in the displacement field is computed by

$$[[\mathbf{u}]] = \mathbf{u}^{\Omega+} - \mathbf{u}^{\Omega-} \tag{9}$$
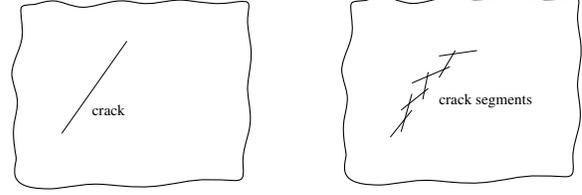
Figure 1: Crack and representation of the crack with crack segments

where the subscript of Ω indicates the different sides of the crack. The jump in the displacement field obviously depends only on $\mathbf{q}_I$:

$$[[\mathbf{u}]](\mathbf{X}) = \sum_{I \in \mathscr{W}_c} 2 \, N_I(\mathbf{X}) \, \mathbf{q}_I \tag{10}$$

where the factor 2 comes from the jump in the step function.

We used the Rankine criterion to generate a crack. The orientation of the crack is perpendicular to the direction of the maximum principal stress. Since the stress around the crack tip is inaccurate especially at crack initiation, we use a rotating crack segment approach where the crack segments are allowed to rotate when the direction of the maximum principal stress changes.

The discrete strain field can be derived as

$$\nabla \mathbf{u}^s(\mathbf{X}) = \sum_{I \in \mathscr{W}} \nabla N_I(\mathbf{X}) \, \mathbf{u}_I + \sum_{I \in \mathscr{W}_c} \nabla N_I(\mathbf{X}) \, \Psi(\mathbf{X}) \, \mathbf{q}_I \tag{11}$$

4 The cohesive law

In the cohesive model, the traction is related to the crack opening, equation (10):

$$t_n = f_t - \frac{f_t}{\delta_{max}} [[u]]_n \text{if} [[u]]_n < \delta_{max}$$
$$\text{and } [[u]]_n^{t+\Delta t} > [[u]]_n^t$$
otherwise $t_n = 0$ when $[[u]]_n^{t+\Delta t} > [[u]]_n^t$ \tag{12}

where

$$[[u]]_n = \mathbf{n} \cdot [[\mathbf{u}]] \tag{13}$$

is the crack opening and δ_{max} is the point where the traction have decayed to zero. Unloading is linear elastic.

Due to its simplicity, we employed the Rankine criterion where the crack is inserted once the maximum principal tensile stress exceeds the tensile strength.

5 Governing equations and discretization

Governing equation is the linear momentum equation. The strong form in a total Lagrangian description is given by

$$\nabla \cdot \mathbf{P} + \rho \mathbf{b} = \rho \ddot{\mathbf{u}} \ \mathbf{X} \in \Omega \qquad (14)$$

where $\mathbf{P}$ is the nominal stress tensor, ρ is the density, $\mathbf{b}$ are body forces and the superimposed dots denote material time derivatives. The displacement and traction boundary conditions are:

$$\mathbf{u} = \bar{\mathbf{u}} \ \mathbf{X} \in \Gamma_u \qquad (15)$$
$$\mathbf{n}_t \cdot \mathbf{P} = \bar{\mathbf{t}} \ \mathbf{X} \in \Gamma_t \qquad (16)$$
$$\mathbf{n}_c \cdot \mathbf{P} = \mathbf{t}_c([[\mathbf{u}]]) \ \mathbf{X} \in \Gamma_c \qquad (17)$$

where the subscript c refers to the crack. The weak form of the linear momentum equation is: Find $\mathbf{u} \in V$ and $\mathbf{v} \in V_0$ such that

$$\delta W = \delta W_{int} - \delta W_{ext} + \delta W_{inertia} + \delta W_{coh} = 0 \quad (18)$$

with

$$\begin{aligned} \delta W_{int} &= \int_\Omega \nabla \mathbf{v} : \mathbf{P} \, d\Omega \\ \delta W_{ext} &= \int_{\Gamma_t} \mathbf{v} \cdot \bar{\mathbf{t}} \, d\Gamma + \int_\Omega \rho \mathbf{v} \cdot \mathbf{b} \, d\Omega \\ \delta W_{inertia} &= \int_\Omega \rho \mathbf{v} \cdot \ddot{\mathbf{u}} \, d\Omega \\ \delta W_{coh} &= \int_{\Gamma_c} [[\mathbf{v}]] \cdot \mathbf{t}_c \, d\Gamma \end{aligned} \qquad (19)$$

where $\mathbf{v}$ are the test functions that have the same structure as the trial functions and V and V_0 are the approximation spaces for the trial and test functions:

$$V = \Big\{ \mathbf{u}(\mathbf{X},t) | \mathbf{u} \in H^1, \ \mathbf{u} = \bar{\mathbf{u}} \text{ on } \Gamma_u, $$
$$\mathbf{u} \text{ discontinuous on } \Gamma_c \Big\}$$
$$\qquad (20)$$
$$V_0 = \Big\{ \mathbf{v} | \mathbf{v} \in H^1, \ \mathbf{v} = 0 \text{ on } \Gamma_u, $$
$$\mathbf{v} \text{ discontinuous on } \Gamma_c \Big\}$$

Substituting $\mathbf{v}$ and $\mathbf{u}$ into the weak form of the linear momentum equation, we obtain

$$\sum_{j=1}^n \int_{\Omega_j} \nabla \mathbf{v}_j : \mathbf{P} \, d\Omega - \sum_{j=1}^n \int_{\Gamma_{t,j}} \mathbf{v} \cdot \bar{\mathbf{t}} \, d\Gamma$$
$$- \sum_{j=1}^n \int_{\Omega_j} \rho \mathbf{v} \cdot \mathbf{b} \, d\Omega + \int_{\Gamma_{c,j}} [[\mathbf{v}]] \cdot \mathbf{t}_c \, d\Gamma$$
$$+ \sum_{j=1}^n \int_{\Omega_j} \rho \mathbf{v} \cdot \ddot{\mathbf{u}} \, d\Omega = 0 \quad (21)$$

With the test and trial functions in eq. (21), the final system of equations is given by:

$$\begin{bmatrix} \mathbf{M}_{IJ}^{uu} & \mathbf{M}_{IJ}^{uq} \\ \mathbf{M}_{IJ}^{qu} & \mathbf{M}_{IJ}^{qq} \end{bmatrix} \cdot \begin{bmatrix} \ddot{\mathbf{u}}_J \\ \ddot{\mathbf{q}}_J \end{bmatrix} = \begin{bmatrix} \mathbf{f}_{I,ext}^u - \mathbf{f}_{I,int}^u \\ \mathbf{f}_{I,ext}^q - \mathbf{f}_{I,int}^q \end{bmatrix} \quad (22)$$

with

$$\mathbf{f}_{I,ext}^u = \int_{\Gamma_t} (\mathbf{N}_I^u)^T \ \mathbf{t} d\Gamma + \int_\Omega (\mathbf{N}_I^u)^T \ \mathbf{b} d\Omega \qquad (23)$$

$$\mathbf{f}_{I,ext}^q = \int_{\Gamma_t} (\mathbf{N}_I^q)^T \ \mathbf{t} d\Gamma + \int_\Omega (\mathbf{N}_I^q)^T \ \mathbf{b} d\Omega$$
$$+ \int_{\Gamma_c} [[(\mathbf{N}_I^q)^T]] \ \mathbf{t}_c d\Gamma \text{ with } \mathbf{N}_I^q = \mathbf{N}_I \ \Psi(\mathbf{X}) \qquad (24)$$

$$\mathbf{f}_{I,int}^u = \int_\Omega (\mathbf{B}_I^u)^T \ \mathbf{P} d\Omega \qquad (25)$$

$$\mathbf{f}_{I,int}^q = \int_\Omega (\mathbf{B}_I^q)^T \ \mathbf{P} d\Omega \text{ with } \mathbf{B}_I^q = \Psi(\mathbf{X}) \nabla \mathbf{N}_I \quad (26)$$

$$\begin{aligned} \mathbf{M}_{IJ}^{uu} &= \mathbf{M}_{IJ}^{qq} = \int_\Omega \rho \mathbf{N}_I \, \mathbf{N}_J^T \, d\Omega \\ \mathbf{M}_{IJ}^{uq} &= \mathbf{M}_{IJ}^{qu} = \int_\Omega \rho \Psi(\mathbf{X}) \, \mathbf{N}_I \, \mathbf{N}_J^T \, d\Omega \end{aligned} \qquad (27)$$

We use stress point integration to evaluate the integrals as explained detailed in Rabczuk and Belytschko (2004).
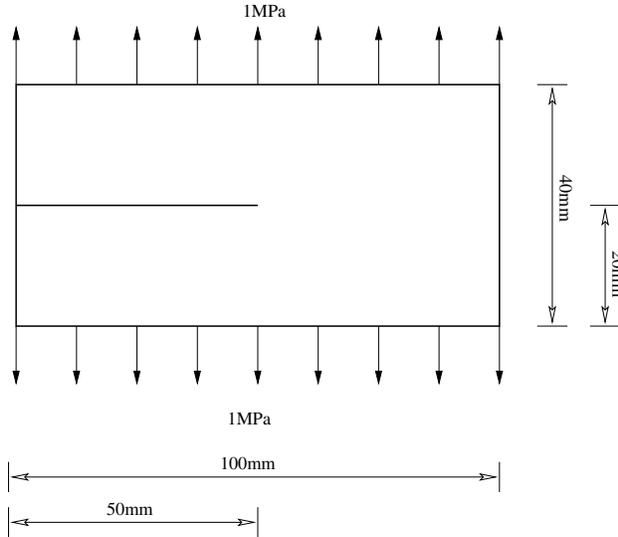
Figure 2: Plate with a horizontal initial notch under tensile tractions

Figure 3: Crack tip speed for the crack branching problem

6 Results

6.1 Crack branching

Let us consider the pre-notched specimen illustrated in figure 2. The specimen is loaded with tensile tractions, $t = 1MPa$, on the both of the top and the bottom edges as a step function in time. Numerical results for this problem have been given by Song, Areais, and Belytschko (2006); Rabczuk and Belytschko (2004); Xu and Needleman (1994) and experimental results with different dimensions are available in Ravi-Chandar (1998); Sharon, Gross, and Fineberg (1995); Fineberg, Sharon, and Cohen (2003). The material properties are: Young's modulus: $E = 32GPa$ and Poisson's ratio $v = 0.20$. The initial Rayleigh wave speed is $c_R = 2119.0m/s$. We modelled the domain with 4,000 and 18,000 nodes using structured and unstructured nodal arrangements. We use explicit time integration with a Courant number of 0.1.

Cracking criterion is Rankine criterion. In contrast to the simulations in Song, Areais, and Belytschko (2006), crack branching occurs naturally. The pattern of crack propagation is shown in figure 4 and the crack tip speed is shown in figure 3. The crack begins to propagate at 15

μs. From this initial phase until crack branching, the crack tip speed increases linearly and peaks at around 20 μs; at this point the crack branches into two cracks. The crack speed drops after branching. Considering the upper branch, we observe an increase in the crack tip speed before the crack branches again. This agrees with the results, which were reported by Sharon, Gross, and Fineberg (1995); Fineberg, Sharon, and Cohen (2003). The numerical simulation finishes at 59 μs shortly before the crack tip reaches the boundary of the specimen, figure 4(b)/(d). The crack pattern is similar to the experimental results reported in References Ravi-Chandar (1998); Sharon, Gross, and Fineberg (1995); Fineberg, Sharon, and Cohen (2003). The basic crack pattern remains even with only 4,000 nodes. However, we found that coarser meshes cannot be used for this problem.

6.2 Mixed mode fracture in a beam under impact loading

An experimental study of mixed mode dynamic crack propagation in concrete beams has been reported by John and Shah (1988). The experimental configuration is shown in figure 5. The thickness of the beam is 0.0254cm and the cross-sectional area is rectangular. It was found that the
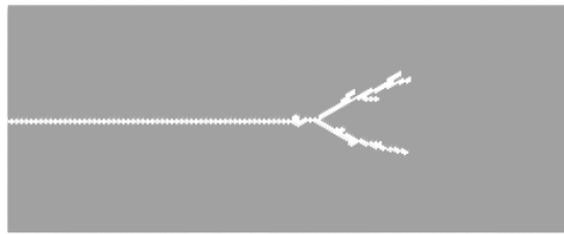
(a) $t = 33\mu s$; 18,000 nodes
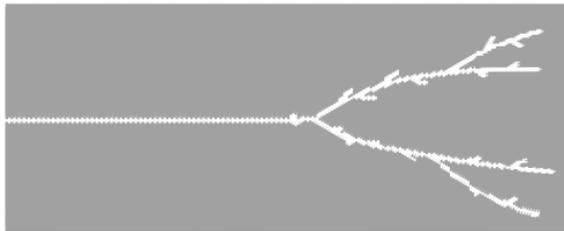
(b) $t = 53\mu s$; 18,000 nodes
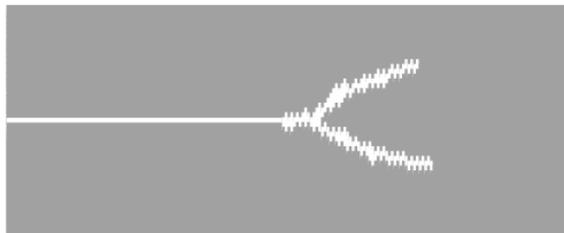
(c) $t = 33\mu s$; 4,000 nodes
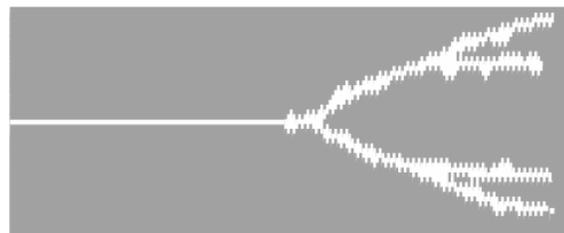
(d) $t = 53\mu s$; 4,000 nodes

Figure 4: Crack pattern in the crack branching problem
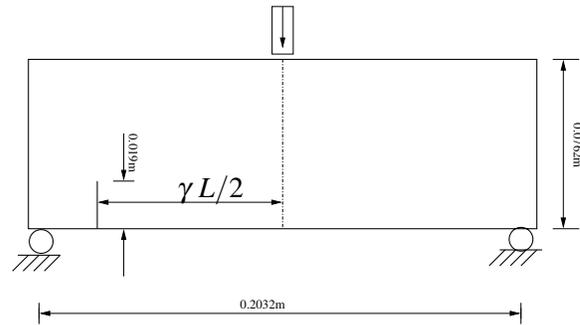
(a)
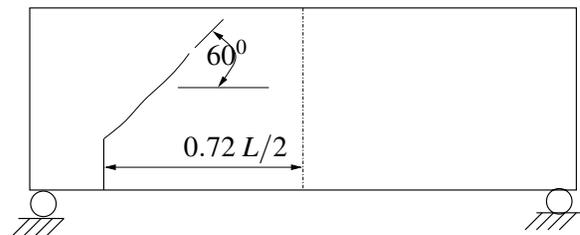
(b)
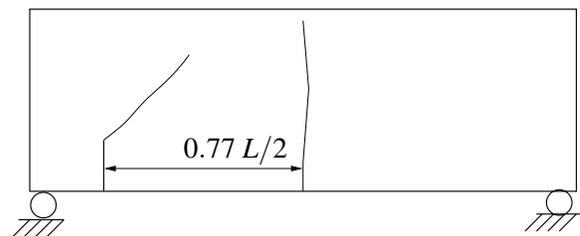
(c)
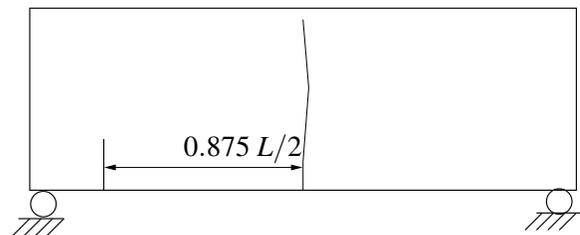
(d)

Figure 5: Test configuration of concrete beam with an offset notch for a mixed mode test and experiment crack configurations for various offset parameters John and Shah (1988): (a) experiment set-up; (b) mixed mode fracture at the initial notch; (c) transition stage; and (d) mode I fracture at the mid-span.

pattern of crack propagation depends mainly on the location of the initial notch characterized by the offset parameter $\gamma = 2d_{notch}/L$ where d_{notch} is the distance between the notch and the mid-span of the beam and L is the span between the supports. For $\gamma = 0$, John and Shah (1988) reported pure mode I fracture, while $\gamma > 0$ can result in either a mode I fracture at the midspan or a mixed mode fracture at the offset notch, figure 5(b/d).

We did simulations with various offset parameters γ to examine the different crack growth trajectories. We assumed plane stress conditions. The material properties are: Young's modulus $E = 31.37$ GPa and Poisson's ratio $\nu = 0.20$. To represent an impact loading, we used a ramp loading instead of a direct impact loading because of a rubber pad which is located between the beam and impact hammer (for more details, refer to References John and Shah (1988)).

Figure 6 shows the numerical results. For $\gamma = 0.7$, the crack propagates only from the offset notch since the stress is released at the mid-span. In this case, the crack propagates at an angle of 52^0, which is in reasonable agreement with the experimental result of 60^0. For the offset notch in the transition zone (i.e. $\gamma = 0.77$), the crack is initiated at the mid-span and both cracks propagate simultaneously. In this simulation, the transition is observed around $\gamma = 0.75$, which is similar to that observed experimentally. Finally, when the offset notch is too far from the loading point and it cannot relax the stress at the mid-span, the crack is initiated at the bottom of the mid-span and propagates as shown in figure 6(d). For all cases, the crack starts to grow at around $620\,\mu s$.

7 Conclusions

We presented a simplified meshless method. The crack is described by a set of cohesive segments that pass through the entire domain of influence of a node. Therefore, there is no need to track the crack path. Complicated problems such as branching cracks can be treated naturally. The method is also simple to implement. The cohesive segments are allowed to rotate after initiation similar to rotating crack models. This removes inaccuracies in the crack pattern caused by inaccu-

(a) *gamma* = 0.7

(b) *gamma* = 0.7

(c) *gamma* = 0.77

(d) *gamma* = 0.8

(e) *gamma* = 0.8
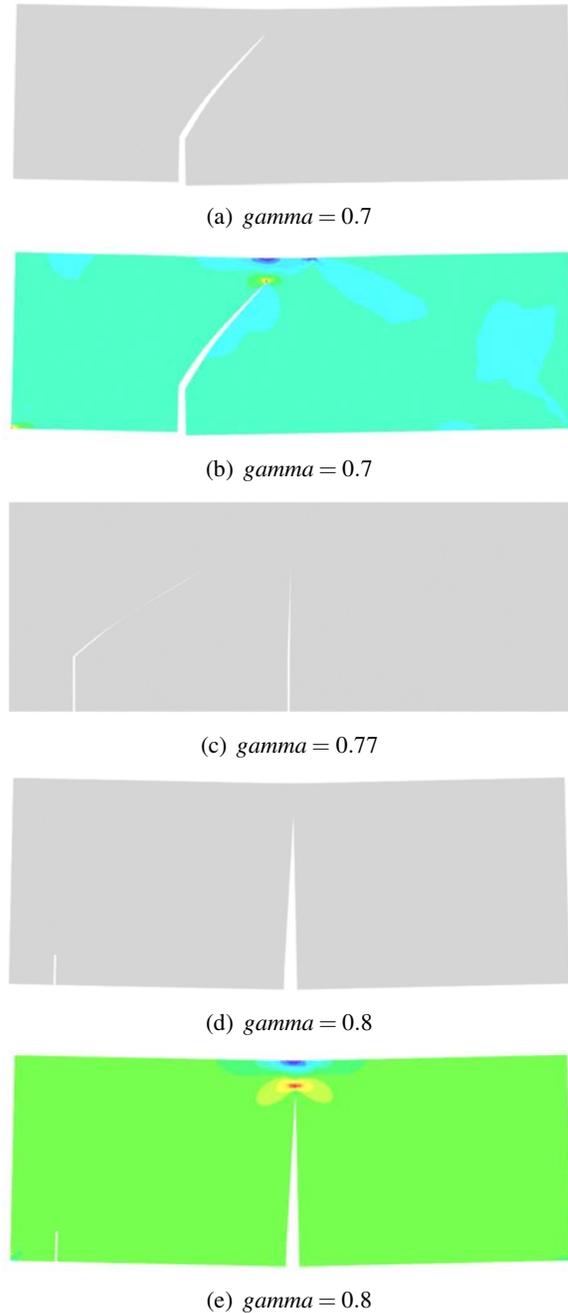
Figure 6: Final crack path for different offset parameters γ

rate stress field that occur once a crack is initiated. We applied the methods to two problems and showed good agreement to experimental results and other more complicated numerical methods. One drawback of the method is that it needs a fine mesh for accurate results. Rabczuk and Belytschko (2007) showed that adaptive methods can alleviate these difficulties. This will be studied in the future. Adaptive node insertion will be implemented that allows crack initiation at any position in the body.

References

Andreaus, U.; Batra, B.; Porfiri, M. (2005): Vibrations of cracked euler-bernoulli beams using meshless local petrov-galerkin (mlpg) method. *CMES: Computer Modeling in Engineering & Sciences*, vol. 9, pp. 111–131.

Atluri, S. (2002): *The Meshless Local Petrov-Galerkin (MLPG) Method*. Tech Science Press.

Atluri, S.; Shen, S. (2002): The meshless local petrov-galerkin method: a simple and less-costly alternative to the finite element and boundary element methods. *Computations and Modelling in Engineering and Sciences*, vol. 3, pp. 11–51.

Atluri, S.; Zhu, T. (1998): A new meshless local petrov-galerkin (mlpg) approach in computational mechanics. *Computational Mechanics*, vol. 22, pp. 117–127.

Atluri, S.; Zhu, T. (2000): The meshless local petrov-galerkin (mlpg) approach for solving problems in elasto-statics. *Computational Mechanics*, vol. 25, pp. 169–179.

Barenblatt, G. (1962): The mathematical theory of equilibrium of cracks in brittle fracture. *Advances in Applied Fracture*, vol. 7, pp. 55–129.

Bazant, Z.; Belytschko, T. (1985): Wave propagation in a strain softening bar: exact solution. *Journal of Engineering Mechanics ASCE*, vol. 11, pp. 381–389.

Bazant, Z.; Oh, B. (1983): Crack band theory for fracture in concrete. *Materials and Structures*, vol. 16, pp. 155–177.

Belytschko, T.; Guo, Y.; Liu, W.; Xiao, S. (2000): A unified stability analysis of mesh-free particle methods. *International Journal for Numerical Methods in Engineering*, vol. 48, pp. 1359–1400.

Belytschko, T.; Krongauz, Y.; Organ, D.; Fleming, M.; Krysl, P. (1996): Meshless methods: An overview and recent developments. *Computer Methods in Applied Mechanics and Engineering*, vol. 139, pp. 3–47.

Belytschko, T.; Lu, Y. (1995): Element-free galerkin methods for static and dynamic fracture. *International Journal of Solids and Structures*, vol. 32, pp. 2547–2570.

Belytschko, T.; Lu, Y.; Gu, L. (1994): Element-free galerkin methods. *International Journal for Numerical Methods in Engineering*, vol. 37, pp. 229–256.

Belytschko, T.; Lu, Y.; Gu, L. (1995): Crack propagation by element-free galerkin methods. *Engineering Fracture Mechanics*, vol. 51, no. 2, pp. 295–315.

Belytschko, T.; Tabbara, M. (1996): Dynamic fracture using element-free galerkin methods. *International Journal for Numerical Methods in Engineering*, vol. 39, no. 6, pp. 923–938.

Chen, Z.; Gan, Y.; Chen, J. (2008): A coupled thermo-mechanical model for simulating the material failure evolution due to localized heating. *CMES: Computer Modeling in Engineering & Sciences*, vol. 26, no. 2, pp. 123–137.

Duarte, C.; Oden, J. (1996): An h-p adaptive method using clouds. *Computer Methods in Applied Mechanics and Engineering*, vol. 139, pp. 237–262.

Fineberg, J.; Sharon, E.; Cohen, G. (2003): Crack front waves in dynamic fracture. *International Journal of Fracture*, vol. 121, pp. 55–69.

Fujimoto, T.; Nishioka, T. (2006): Numerical simulation of dynamic elasto visco-plastic fracture using moving finite element method. *CMES: Computer Modeling in Engineering & Sciences*, vol. 11, no. 2, pp. 91–101.

Gao, L.; Liu, K.; Liu, Y. (2006): Applications of mlpg method in dynamic fracture problems. *CMES: Computer Modeling in Engineering & Sciences*, vol. 12, no. 3, pp. 181–195.

Guo, Y.; Nairn, J. (2006): Three-dimensional dynamic fracture analysis using the material point method. *CMES: Computer Modeling in Engineering & Sciences*, vol. 16, no. 3, pp. 141–155.

Guz, A.; Menshykov, O.; Zozulya, V. (2007): Contact problem for the flat elliptical crack under normally incident shear wave. *CMES: Computer Modeling in Engineering & Sciences*, vol. 17, no. 3, pp. 205–214.

Haasemann, G.; Kastner, M.; Ulbricht, V. (2006): Multi-scale modelling and simulation of textile reinforced materials. *CMC: Computers Materials & Continua*, vol. 3, no. 3, pp. 131–145.

Hagihara, S.; Tsunori, M.; Ikeda, T. (2007): Application of meshfree method to elastic-plastic fracture mechanics parameter analysis. *CMES: Computer Modeling in Engineering & Sciences*, vol. 17, no. 2, pp. 63–72.

Han, Z.; Atluri, S. (2003): Truly meshless local petrov-galerkin (mlpg) solutions of traction and displacement bies. *Computations and Modelling in Engineering and Sciences*, vol. 4, pp. 665–678.

Han, Z.; Atluri, S. (2004): A meshless local petrov-galerkin (mlpg) approach for 3-dimensional elasto-dynamics. *CMC: Computers Materials & Continua*, vol. 2, no. 1, pp. 129–140.

Han, Z.; Liu, H.; Rajendran, A.; Atluri, S. (2007): The applications of meshless local petrov-galerkin (mlpg) approaches in high-speed impact, penetration and perforation problems. *CMES: Computer Modeling in Engineering & Sciences*, vol. 14, pp. 119–128.

Hao, S.; Liu, W. (2006): Moving particle finite element method with superconvergence: Nodal integration formulation and applications. *Computer Methods in Applied Mechanics and Engineering*, vol. 195, no. 44-47, pp. 6059–6072.

Hao, S.; Liu, W.; Chang, C. (2000): Computer implementation of damage models by finite element and meshfree methods. *Computer Methods in Applied Mechanics and Engineering*, vol. 187, no. 3-4, pp. 401–440.

Hao, S.; Liu, W.; Klein, P.; Rosakis, A. (2004): Modeling and simulation of intersonic crack growth. *International Journal of Solids and Structures*, vol. 41, no. 7, pp. 1773–1799.

Hao, S.; Liu, W.; Qian, D. (2000): Localization-induced band and cohesive model. *Journal of Applied Mechanics-Transactions of the ASME*, vol. 67, no. 4, pp. 803–812.

Hillerborg, A.; Modeer, M.; Peterson, P. E. (1976): Analysis of crack formation and crack growth in concrete by means of fracture mechanics and finite elements. *Cement and Concrete Research*, vol. 6, pp. 773–782.

Idelsohn, S.; Onate, E.; Pin, F. D. (2004): The particle finite element method: a powerful tool to solve incompressible flows with free surfaces and breaking waves. *International Journal for Numerical Methods in Engineering*, vol. 61, pp. 964–989.

Jirasek, M.; Zimmermann, T. (1998): Analysis of rotating crack model. *Journal of Engineering Mechanics*, vol. 124, pp. 842–851.

John, R.; Shah, S. (1988): Mixed mode fracture of concrete subjected to impact loading. *Journal of Structural Engineering (ASCE)*, vol. 116, pp. 585–602.

Le, P.; Mai-Duy, N.; Tran-Cong, T. (2008): A meshless modeling of dynamic strain localization in quasi-brittle materials using radial basis function networks. *CMES: Computer Modeling in Engineering & Sciences*, vol. 25, no. 1, pp. 43–67.

Li, S.; Simonson, B. C. (2003): Meshfree simulation of ductile crack propagation. *International Journal of Computational Methods in Engineering Science and Mechanics*, vol. 6, pp. 1–19.

Liu, H.; Han, Z.; Rajendran, A.; Atluri, S. (2006): Computational modeling of impact response with the rg damage model and the meshless local petrov-galerkin (mlpg) approaches. *Computers Materials and Continua*, vol. 4, pp. 43–53.

Liu, K.; Long, S.; Li, G. (2008): A meshless local petrov-galerkin method for the analysis of cracks in the isotropic functionally graded material. *CMC: Computers Materials & Continua*, vol. 7, no. 1, pp. 43–57.

Liu, W.; Hao, S.; Belytschko, T. (1999): Multiple scale meshfree methods for damage fracture and localization. *Computational Material Science*, vol. 16, no. 1-4, pp. 197–205.

Liu, W.; Jun, S.; Zhang, Y. (1995): Reproducing kernel particle methods. *International Journal for Numerical Methods in Engineering*, vol. 20, pp. 1081–1106.

Ma, J.; Lu, H.; Wang, B. (2006): Multiscale simulation using generalized interpolation material point (gimp) method and molecular dynamics (md). *CMES: Computer Modeling in Engineering & Sciences*, vol. 14, no. 2, pp. 101–117.

Mai-Duy, N.; Khennane, A.; Tran-Cong, T. (2007): Computation of laminated composite plates using integrated radial basis function networks. *CMC: Computers Materials & Continua*, vol. 5, no. 1, pp. 63–77.

Malvar, L.; Fourney, M. (1990): A three dimensional application of the smeared crack approach. *Engineering Fracture Mechanics*, vol. 35, no. 1-3, pp. 251–260.

Melenk, J. M.; Babuska, I. (1996): The partition of unity finite element method: basic theory and applications. *Computer Methods in Applied Mechanics and Engineering*, vol. 139, pp. 289–314.

Nguyen-Van, H.; N, N. M.-D.; Tran-Cong, T. (2008): A smoothed four-node piezoelectric element for analysis of two-dimensional smart structures. *CMES: Computer Modeling in Engineering & Sciences*, vol. 23, no. 3, pp. 209–222.

Nishioka, T.; Kobayashi, Y.; Fujimoto, T. (2007): The moving finite element method based on delaunay automatic triangulation for fracture path prediction simulations in nonlinear elastic-plastic materials. *CMES: Computer Modeling in Engineering & Sciences*, vol. 17, no. 3, pp. 231–238.

Nishioka, T.; Tchouikov, S.; Fujimoto, T. (2006): Numerical investigation of the multiple dynamic crack branching phenomena. *CMC: Computers Materials & Continua*, vol. 3, no. 3, pp. 147–153.

Organ, D.; Fleming, M.; Terry, T.; Belytschko, T. (1996): Continuous meshless approximations for nonconvex bodies by diffraction and transparency. *Computational Mechanics*, vol. 18, pp. 225–235.

Rabczuk, T.; Areias, P. (2006): A meshfree thin shell for arbitrary evolving cracks based on an extrinsic basis. *CMES: Computer Modeling in Engineering & Sciences*, vol. 16, no. 2, pp. 115–130.

Rabczuk, T.; Areias, P.; Belytschko, T. (2007): A meshfree thin shell method for non-linear dynamic fracture. *International Journal for Numerical Methods in Engineering*, vol. 72, pp. 524–548.

Rabczuk, T.; Areias, P.; Belytschko, T. (2007): A simplified mesh-free method for shear bands with cohesive surfaces. *International Journal for Numerical Methods in Engineering*, vol. 69, pp. 993–1021.

Rabczuk, T.; Belytschko, T. (2004): Cracking particles: A simplified meshfree method for arbitrary evolving cracks. *International Journal for Numerical Methods in Engineering*, vol. 61, no. 13, pp. 2316–2343.

Rabczuk, T.; Belytschko, T. (2005): Adaptivity for structured meshfree particle methods in 2d and 3d. *International Journal for Numerical Methods in Engineering*, vol. 63, no. 11, pp. 1559–1582.

Rabczuk, T.; Belytschko, T. (2006): Application of particle methods to static fracture of rein-

forced concrete structures. *International Journal of Fracture*, vol. 137, no. 19-49, pp. 1559–1582.

Rabczuk, T.; Belytschko, T. (2007): A three dimensional large deformation meshfree method for arbitrary evolving cracks. *Computer Methods in Applied Mechanics and Engineering*, vol. 196, pp. 2777–2799.

Rabczuk, T.; Belytschko, T.; Xiao, S. (2004): Stable particle methods based on lagrangian kernels. *Computer Methods in Applied Mechanics and Engineering*, vol. 193, pp. 1035–1063.

Rabczuk, T.; Eibl, J. (2003): Simulation of high velocity concrete fragmentation using sph/mlsph. *International Journal for Numerical Methods in Engineering*, vol. 56, pp. 1421–1444.

Rabczuk, T.; Zi, G. (2007): A meshfree method based on the local partition of unity for cohesive cracks. *Computational Mechanics*, vol. 39, no. 6, pp. 743–760.

Randles, P.; Libersky, L. (1997): Recent improvements in sph modeling of hypervelocity impact. *International Journal of Impact Engineering*, vol. 20, pp. 525–532.

Ravi-Chandar, K. (1998): Dynamic fracture of nominally brittle materials. *International Journal of Fracture*, vol. 90, pp. 83–102.

Sharon, E.; Gross, P.; Fineberg, J. (1995): Local crack branching as a mechanism for instability in dynamic fracture. *Physical Review Letters*, vol. 74, pp. 5096–5099.

Shen, S.; Atluri, S. (2005): A tangent stiffness mlpg method for atom/continuum multiscale simulation. *CMES: Computer Modeling in Engineering & Sciences*, vol. 7, pp. 49–67.

Sladek, J.; Sladek, V.; Krivacek, J. (2005): Meshless local petrov-galerkin method for stress and crack analysis in 3-d axisymmetric fgm bodies. *CMES: Computer Modeling in Engineering & Sciences*, vol. 8, no. 3, pp. 259–270.

Sladek, J.; Sladek, V.; Zhang, C. (2007): Fracture analyses in continuously nonhomogeneous piezoelectric solids by the mlpg. *CMES: Computer Modeling in Engineering & Sciences*, vol. 19, no. 3, pp. 247–262.

Sladek, J.; V. Sladek, V.; Zhang, C. (2007): Application of the mlpg to thermo-piezoelectricity. *CMES: Computer Modeling in Engineering & Sciences*, vol. 22, pp. 217–233.

Song, J.-H.; Areais, P.; Belytschko, T. (2006): A method for dynamic crack and shear band propagation with phantom nodes. *International Journal for Numerical Methods in Engineering*, vol. 67, pp. 868–893.

Tang, Z.; Shen, S.; Atluri, N. (2003): Analysis of materials with strain-gradient effects: A meshless local petrov-galerkin(mlpg) approach, with nodal displacements only. *Computations and Modelling in Engineering and Sciences*, vol. 4, pp. 177–196.

Wen, P.; Hon, Y. (2007): Geometrically nonlinear analysis of reissner-mindlin plate by meshless computation. *CMES: Computer Modeling in Engineering & Sciences*, vol. 21, pp. 177–191.

Wu, C.; Liu, K. (2007): A state space approach for the analysis of doubly curved functionally graded elastic and piezoelectric shells. *CMC: Computers Materials & Continua*, vol. 6, no. 3, pp. 177–199.

Wu, X.; Tao, S. S. W. (2007): Meshless local petrov-galerkin collocation method for two-dimensional heat conduction problems. *CMES: Computer Modeling in Engineering & Sciences*, vol. 22, pp. 65–76.

Xu, X.; Needleman, A. (1994): Numerical simulations of fast crack growth in brittle solids. *Journal of the Mechanics and Physics of Solids*, vol. 42, pp. 1397–1434.

Zi, G.; Rabczuk, T.; Wall, W. (2007): Extended meshfree methods without branch enrichment for cohesive cracks. *Computational Mechanics*, vol. 40, pp. 367–382.

Zimmermann, T. (1986): Failure and fracturing analysis of concrete structures. *Nuclear Engineering and Design*, vol. 92, no. 3, pp. 389–410.